

Detection of neutral atoms sputtered from ion-bombarded single-crystal surfaces Rh{111} and $p(2 \times 2)$ O/Rh{111}: Ejection mechanism and surface structure determinations from energy- and angle-resolved measurements

J. Singh,^{a)} C. T. Reimann, J. P. Baxter,^{b)} G. A. Schick,^{c)} P. H. Kobrin,^{d)} B. J. Garrison, and N. Winograd

Department of Chemistry, Pennsylvania State University, University Park, Pennsylvania 16802

(Received 1 October 1986; accepted 29 December 1986)

A temporally sensitive ionization scheme is used in conjunction with a position-sensitive detector to measure simultaneously energy- and angle-resolved distributions of sputtered neutral atoms. We report results for 5-keV Ar⁺ ion-bombarded Rh{111} single-crystal surfaces, both clean and with a $p(2 \times 2)$ overlayer of oxygen atoms. The angular distributions and their variation with ejection kinetic energy are shown to give information about simple collision sequences that produce directionally preferential atom ejection. The changes that occur in the ejection distributions upon O atom adsorption suggest that O atoms occupy the "expected" sites, the sites that would be occupied by Rh atoms in a new monolayer.

I. INTRODUCTION

Secondary ion mass spectrometry (SIMS) is a popular surface analysis technique due to the sensitivity with which ions can be detected and mass analyzed. Traditional applications of the SIMS technique include trace analysis and depth profiling. A more novel application of SIMS is in the determination of surface structure through the use of angle-resolved measurements in conjunction with classical dynamics simulations of the ion-bombardment process.¹ In this respect SIMS has been used to determine adsorption sites on single-crystal surfaces.² However, the technique is limited by the dependence of ion ejection yields on the electronic properties of the matrix.³ In addition, the extraction of surface structural information is hampered by difficulties in modeling the ionization process.⁴ It would, therefore, be advantageous to monitor desorbing neutral material. The total ejection yield is typically dominated by neutral species, and the dependence of the neutral yield on various experimental parameters is generally much less pronounced than that of the ion yield. Angle-resolved measurements of neutral material desorbing from ion-bombarded surfaces are, therefore, applicable to a wider range of surface compositions and are more easily modeled for use in determining surface structure and ejection mechanisms.^{5,6}

Although neutral sputtering measurements should provide more easily interpretable information on ejection mechanisms, many factors have hampered work along these lines. Neutral atoms are difficult to detect efficiently. Also, poor vacuum conditions and high doses of incident ions for sputtering cause the surfaces on which such experiments are performed to be poorly characterized.

In the present work we have employed multiphoton resonance ionization (MPRI) as a detection method to increase the neutral detection efficiency.⁵ We have measured simultaneously energy- and angle-resolved distributions of neutral Rh atoms desorbing from Rh{111} and $p(2 \times 2)$ O/Rh{111} single-crystal surfaces.⁷ The independently resolved energy and angle distributions provide semiquantita-

tive information on the sputtering mechanisms that take place in the near surface region of a single crystal that is bombarded by low-energy heavy ions. Moreover, a comparison of molecular dynamics simulations to the experimentally measured distributions from $p(2 \times 2)$ O/Rh{111} allows determination of the location of the O atoms on the Rh{111} surface.⁸

II. EXPERIMENT

The details of our experimental setup to measure energy- and angle-resolved neutral atom ejection distributions have been described previously.⁹ Briefly, a pulsed ion beam is focused to a 1–2 mm² spot on the sample. As sputtered atoms eject away from the point of impact, a cylindrically focused laser pulse is directed about 1 cm away from the target, ionizing a "slice" of the sputtered cloud. The ionization is accomplished by a two-photon (312.4-nm) process involving a resonant intermediate energy level. The ions are extracted by an electric field and imaged onto a multichannel plate (MCP). The polar angular distribution of the sputtered atoms before ionization is extracted from the spatial spread of signal detected on the MCP. The time delay (of the order of several μ s) between the incident ion pulse (≈ 200 ns wide) and the laser pulse (≈ 6 ns wide) defines the kinetic energies of the particles ionized by the laser and is varied to produce the energy-resolved distributions. For a given time delay, different portions of the MCP image correspond to different kinetic energies as well as to different polar ejection angles, but deconvolution of a series of MCP images taken using different time delays gives separately resolved energy and angle distributions of the sputtered atoms.

The vacuum chamber has a base pressure of 2×10^{-10} Torr, so that contamination of the Rh{111} sample during a sequence of measurements is not significant. The fluence of 5-keV Ar⁺ incident on the sample during a measurement was about 2×10^{12} ions/cm², corresponding to "static mode" bombardment with negligible destruction of the surface during the course of the measurements. The Rh{111}

crystal was cleaned by previously published methods.¹⁰ The $p(2 \times 2)$ O/Rh{111} structure was generated by exposing a clean Rh{111} surface to 10 L of oxygen. The cleanliness and structural integrity of the Rh{111} surface were monitored using LEED and Auger spectroscopy.

III. RESULTS AND DISCUSSION

The energy- and angle-resolved neutral-particle (EARN) measurements of sputtered Rh atoms ejecting from both clean and oxygen-covered surfaces were made in the $+30^\circ$, -30° , and 0° azimuthal directions, which are defined in the inset of Fig. 1(a). The EARN distributions are displayed in Fig. 1(a) for the $+30^\circ$ azimuth (positive θ values) and the -30° azimuths (negative θ values). The off-normal intensity for the 0° azimuths (not shown here) is generally less than that for either the $\pm 30^\circ$ azimuths. Thus, there is strong preferred ejection toward the open channels of the crystal surfaces, as has been observed by previous energy-integrated angular distribution measurements.¹¹

The significant feature observed here and in our recent studies^{7,12} is that the observed angular distributions vary sys-

tematically with the kinetic energy of the particles. Sections through the energy-angle surface of Fig. 1(a) are shown in Fig. 1(b) for different kinetic energy ranges. For low kinetic energies, 5–10 eV, the polar angular pattern has dissimilar distributions for the $+30^\circ$ and -30° azimuthal directions, indicating threefold symmetry. This dissimilarity suggests that at least the first two monolayers of the crystal interact during the time required to eject low-energy particles, since only by including at least the first two monolayers is threefold structural symmetry obtained. Examination of classical dynamics simulations of sputtering trajectories reveals that the higher ejection yield in the -30° azimuth relative to the $+30^\circ$ azimuth occurs because a second-layer atom knocks a first-layer atom much more easily in the -30° azimuthal direction, as is apparent in the inset of Fig. 1(a).⁸ In the $+30^\circ$ azimuthal direction, by contrast, the relevant second-layer atom is too far away to effectively knock out a first-layer atom in that direction.

For high kinetic energies, 20–50 eV, the polar angle distributions for the $+30^\circ$ and -30° azimuthal directions are much more similar in intensity, so that a sixfold symmetry is approached. This suggests that energetic ejections are caused by collisions involving the first monolayer only. Also, energetic particles are emitted very early in the collision cascade, before second-layer atoms have had a chance to become involved in particle ejection. The approximate sixfold symmetry is due to the focusing effect of pairs of surface atoms with "open" directions along the $\pm 30^\circ$ azimuthal directions.

Another feature of the data in Fig. 1(b) is that the amount of normal ejection relative to the amount of off-normal ejection increases as the kinetic energy increases. This enhancement at high kinetic energy can be explained by classical dynamics simulations.⁸ An incident ion may be channeled to the third layer or even deeper without losing much energy in collisions. A subsequent hard reflection followed by an impact with a second-layer atom may cause the second-layer atom to be channeled by three adjacent surface atoms straight out in the normal direction. On the other hand, lower kinetic energy ejected atoms are probably the result of collisions which have occurred after a considerable amount of momentum has already been dissipated. Thus the atoms are less likely to be moving in the normal direction.

Molecular oxygen has been shown to undergo dissociative chemisorption to form a $p(2 \times 2)$ oxygen overlayer on clean Rh{111}.¹³ The EARN distribution of Rh atoms sputtered from this system was measured, and the resulting polar angular distributions for the clean and oxygen-covered cases for both low and high kinetic energy ranges are shown in Fig. 2.

At low kinetic energies, the addition of a layer of oxygen causes the off-normal ejection peaks to occur at angles closer to the normal direction. Also, the off-normal ejection peak in the -30° azimuthal direction is diminished relative to the corresponding peak in the $+30^\circ$ azimuthal direction. At high kinetic energy the off-normal ejection peaks for the $\pm 30^\circ$ azimuthal directions are both attenuated by about the same amount relative to the normal peak, and the peak polar angle positions do not shift very much.

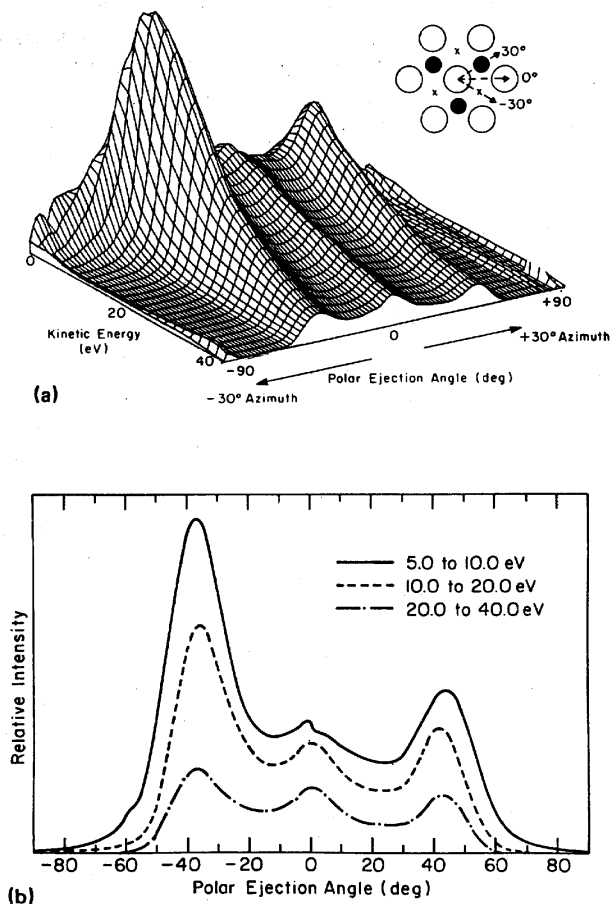


FIG. 1. (a) Kinetic energy and polar ejection angle distributions of ejected neutral Rh atoms in the $\pm 30^\circ$ azimuthal directions. The inset defines these azimuthal directions relative to the surface Rh atoms (open circles) and the second-layer atoms (closed circles). The symbol \times marks the expected adsorption site on the surface, which is the place where a Rh atom would reside in the next Rh monolayer. (b) Polar angle distributions of ejected neutral Rh atoms integrated over low, medium, and high ejection kinetic energy ranges. Note, a polar ejection angle of 0° corresponds to normal ejection.

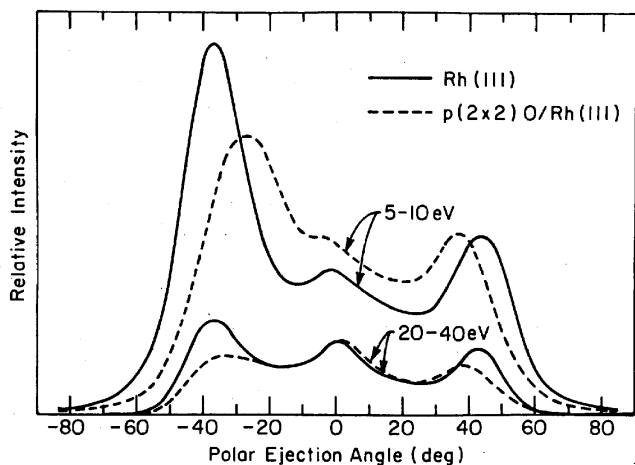


FIG. 2. Polar angle distributions of ejected neutral Rh atoms for clean Rh{111} and for $p(2 \times 2)$ O/Rh{111} systems. The distributions are integrated over low and high ejection kinetic energy ranges.

The greater decrease in the off-normal ejection for the -30° azimuthal direction is consistent with O atoms occupying the "C" or "expected" site on the surface, which places the O atom along the -30° direction with respect to a surface Rh atom [at the position of the \times 's in the inset to Fig. 1(a)]. Molecular dynamics simulations show better agreement with experiments when O was assumed to be in the threefold hollow expected sites than when O was assumed to be in the atop sites.⁸ Recent dynamical LEED studies¹⁴ also indicate that O occupies the expected site.

This C-site location might explain why the off-normal ejection peak in the -30° direction moves closer to normal ejection, since a Rh atom must be ejected closer to the normal direction to escape over the O atom. On the other hand, the shift in the peak in the $+30^\circ$ direction is at present unexplained. The small shift in the off-normal ejection peak angles at high kinetic energy is explained by the smaller interaction cross section between Rh and O when Rh has a higher velocity.

The continued prominence of normal ejection relative to off-normal ejection at high kinetic energies is also consistent with O lying in the C site. If O were assumed to lie in the B site, which is the threefold hollow site directly above a second-layer Rh atom, then by the mechanism suggested earlier for energetic normal ejection, the normal peak would be predicted to become relatively smaller upon adsorption of O atoms, whereas instead the off-normal peak became smaller.

IV. CONCLUSIONS

An understanding of the details of the sputtering process in the test case of a single-crystal substrate with and without an ordered adsorbate overlayer lays the groundwork for applications to other systems. Our preliminary work on

Rh{111} and $p(2 \times 2)$ O/Rh{111} involving efficient neutral Rh detection by MPRI shows that analysis of sputtering distributions yields semiquantitative information about surface structure. Such information can be used to extract ejection mechanisms, surface symmetry, and adsorbate location. It should be noted further that the MPRI technique can be used to selectively ionize a variety of types of atoms, both in the ground state and in the excited state. We are currently pursuing EARN distributions for adsorbate material. Adsorbate location would be considerably easier to ascertain if the adsorbate atoms were observed directly. Thus, the technique promises to have future applications.

ACKNOWLEDGMENTS

The authors are grateful for the financial support of the National Science Foundation, the Office of Naval Research, and the Air Force Office of Scientific Research. Barbara J. Garrison also appreciates financial support from the IBM Corporation and the Camille and Henry Dreyfus Foundation.

^{a)} Present address: Department of Physics and Astronomy, 177 Chemistry-Physics Building, University of Kentucky, Lexington, KY 40506-0055.

^{b)} Present address: University of Maine, 9 Barrows Hall, Orono, ME 04469-0107.

^{c)} Present address: Center for Molecular Electronics, Carnegie-Mellon University, 4400 Fifth Avenue, Pittsburgh, PA 15213.

^{d)} Present address: Rockwell Science Center, P. O. Box 1085, Thousand Oaks, CA 91360.

¹⁾ N. Winograd, *Chemical Physics*, Springer Ser. No. 35 (Springer, New York, 1984), p. 403.

²⁾ R. A. Gibbs, S. P. Holland, K. E. Foley, B. J. Garrison, and N. Winograd, *J. Chem. Phys.* **76**, 684 (1982).

³⁾ F. M. Kimock, D. L. Pappas, and N. Winograd, *Anal. Chem.* **57**, 2669 (1985); H. T. Jonkman and J. Michl, *J. Am. Chem. Soc.* **103**, 733 (1981); H. Grade and R. G. Cooks, *ibid.* **100**, 5615 (1978).

⁴⁾ M. L. Yu, *Phys. Rev. Lett.* **40**, 574 (1978); J. K. Norskov and B. I. Lundqvist, *Phys. Rev. B* **19**, 5661 (1979); Z. Sroubek, K. Zdansky, and J. Zavadil, *Phys. Rev. Lett.* **45**, 580 (1980).

⁵⁾ F. M. Kimock, J. P. Baxter, D. L. Pappas, P. H. Koblin, and N. Winograd, *Anal. Chem.* **56**, 2782 (1984); G. S. Hurst, M. G. Payne, S. D. Kramer, and J. P. Young, *Rev. Mod. Phys.* **51**, 767 (1979); J. E. Parks, H. W. Schmitt, G. S. Hurst, and W. M. Fairbank, Jr., *Thin Solid Films* **108**, 69 (1983).

⁶⁾ B. J. Garrison, *Surf. Sci.* **167**, L225 (1986).

⁷⁾ N. Winograd, P. H. Koblin, G. A. Schick, J. Singh, J. P. Baxter, and B. J. Garrison, *Surf. Sci.* **176**, L817 (1986).

⁸⁾ B. J. Garrison and D. E. Harrison (to be published).

⁹⁾ P. H. Koblin, G. A. Schick, J. P. Baxter, and N. Winograd, *Rev. Sci. Instrum.* **57**, 1354 (1986).

¹⁰⁾ L. A. DeLouise and N. Winograd, *Surf. Sci.* **138**, 417 (1984).

¹¹⁾ G. K. Wehner, *J. Appl. Phys.* **26**, 1056 (1955); M. T. Robinson and A. L. Southern, *ibid.* **38**, 2969 (1967); W. Szymczak and K. Wittmaack, *Nucl. Instrum. Methods* **194**, 561 (1982).

¹²⁾ J. P. Baxter, G. A. Schick, J. Singh, P. H. Koblin, and N. Winograd, *J. Vac. Sci. Technol. A* **4**, 1218 (1986).

¹³⁾ P. A. Thiel, J. T. Yates, Jr., and W. H. Weinberg, *Surf. Sci.* **82**, 22 (1979).

¹⁴⁾ P. C. Wong, K. C. Hui, M. Y. Zhou, and K. A. R. Mitchell, *Surf. Sci.* **165**, L21 (1986).